

# IceCube: Spaceflight Demonstration of 883-GHz Cloud Radiometer for Future Science

Dong L. Wu<sup>a</sup>, Jeffrey R. Piepmeier<sup>a</sup>, Jaime Esper<sup>a</sup>, Negar Ehsan<sup>a</sup>, Paul E. Racette<sup>a</sup>, Thomas E. Johnson<sup>a</sup>, Brian S. Abresch<sup>a</sup>, and Eric Bryerton<sup>b</sup>

<sup>a</sup>NASA Goddard Space Flight Center (GSFC)  
Greenbelt, Maryland, USA; <sup>b</sup>Virginia Diodes, Inc. (VDI)  
Charlottesville, Virginia, USA

## ABSTRACT

Cloud ice play important roles in Earth's climate and weather systems through their interactions with atmospheric radiation, dynamics, energy and precipitation processes. Submillimeter (submm) wave remote sensing at 200-1000 GHz is able to provide the sensitivity not covered by visible (VIS)/infrared (IR) and low-frequency microwave (MW) sensors (10-183 GHz), and measure cloud ice in the middle-to-upper troposphere. The IceCube 883-GHz cloud radiometer is the latest of NASA's efforts to advance the technology readiness level (TRL) of submm-wave receiver technology for future compact, low-cost implementation of Earth observing systems. Emerging CubeSat opportunities allow a fast-track development and spaceflight demonstration of IceCube on a 3-U CubeSat. Funded by NASA's In-Space Validation of Earth Science Technologies (InVEST) program and Science Mission Directorate (SMD), IceCube is the first CubeSat developed and flown by Goddard Space Flight Center (GSFC) in 2.5 years, using commercial off-the-shelf (COTS) components and subsystems. It was successfully released from International Space Station (ISS) in May 2017, acquired 15-month science data and produced the first global map of the 883-GHz cloud ice. It achieved all mission objectives and provided a pathway for future cost-effective cloud observations from CubeSat constellation.

**Keywords:** Submm-wave remote sensing, cloud ice, CubeSat, constellation, ISS

## 1. INTRODUCTION

The primary objective of IceCube is to raise the TRL of a commercial 883-GHz cloud radiometer from 5 to 7 by flying and validating the technology in a relevant spaceflight environment. Successful demonstration of the commercial 883-GHz cloud radiometer reduces the risks and costs of future Earth Science missions on cloud ice observations. As shown in Fig.1, Submm wave remote sensing has the advantage of filling the sensitivity gap between MW and VIS/IR remote sensing. The technique provides adequate ice cloud penetration as well as sensitivity to cloud ice mass and microphysical properties in the middle-to-upper troposphere. A combination of IR, mm- and submm-wave cloud radiometers can provide a complete observation of cloud systems [1][2]. For ice cloud observations, the 860-900 GHz spectral window provides not only good sensitivity to cloud scattering but also adequate penetration to the cloud for cloud ice measurements. Cloud observations at 1-5 THz becomes difficult because of the increasing atmospheric attenuation from continuum absorption.

Ice water path (IWP) is a key parameter to characterize cloud radiative and hydrological properties. Despite great advances from CloudSat radar and other satellite sensors [3], global IWP measurements still differ from each other by a factor of 2 or greater, largely because of uncertainties about the microphysical property assumptions used in cloud ice retrieval algorithms [4][5]. To improve cloud ice measurements, GSFC has been working with Virginia Diodes, Inc. (VDI) to develop receivers that span from 100 GHz to 1 THz, which has become the foundation of GSFC's airborne Compact Scanning Submillimeter-wave Imaging Radiometer (CoSSIR) [6]. Designed as both a conical and cross-track imager with six receivers centered at 183, 220, 380, 640 V&H, and 874 GHz and eleven channels, CoSSIR was flown on NASA's ER-2 aircraft, which became the precursor of IceCube.

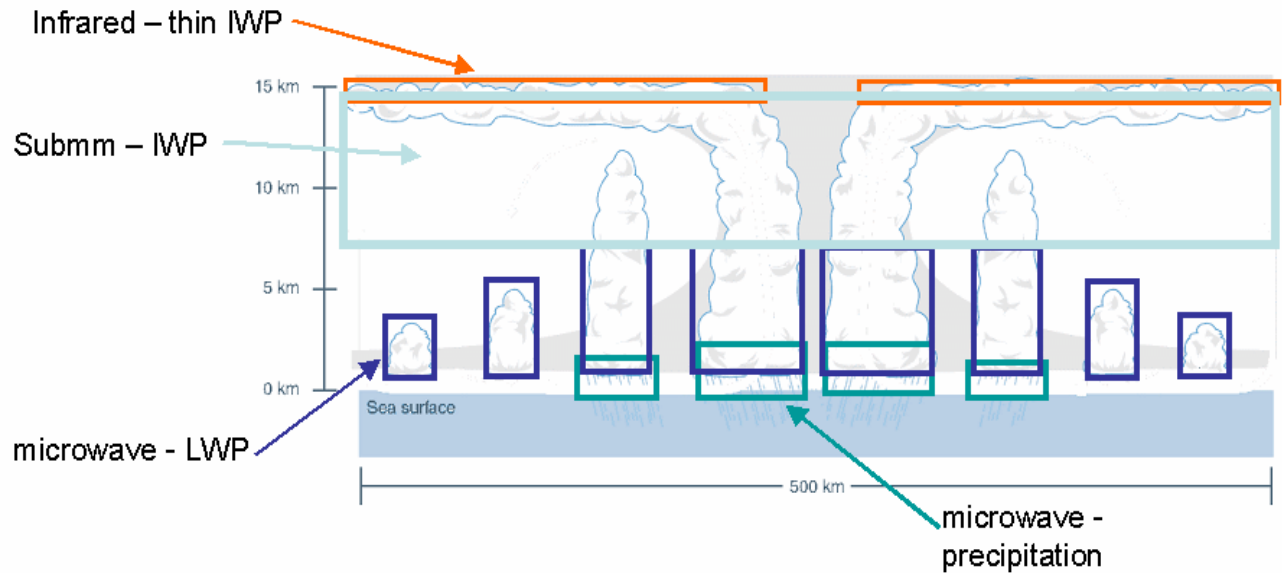


Fig.1. Submm-wave sensors provide sensitivity of cloud ice water path (IWP) in the region that is not covered by current satellite IR and microwave (MW) observations. The contribution from submm-wave sensors can fill the gap in cloud observations (i.e., cloud optical thickness and effective particle size from IR/visible; precipitation and cloud liquid water path (LWP) from low-frequency microwave).

### 1.1 Measurement Technique

MW radiation as seen from space is primarily from the Earth's surface and atmospheric gases. There are spectral windows where no major absorption lines from atmospheric gases are present in the spectrum. Both the Earth's surface and atmospheric gases radiate like a grey body (blackbody with imperfect emissivity  $\epsilon$ ), which produces a MW radiance characterized by a brightness temperature ( $T_b$ ).  $T_b$  can be related to the physical temperature ( $T$ ) of the emission source ( $T_b = \epsilon T$ ) and is typically warmer if it is near the surface and colder if it is from the upper troposphere. In the presence of ice clouds, MW radiation will be scattered by the clouds in all directions. The scattered  $T_b$  is generally lower than the clear-sky  $T_b$  at nadir viewing from space, because it is a combination of upwelling warm  $T_b$  and downwelling cold space background (i.e., Cosmic Microwave Background, or CMB). The  $T_b$  of CMB is 2.73K at 0.1 GHz but becomes nearly zero at 883 GHz from Planck's black-body equation.

The effects of cloud scattering on MW radiance is shown in Fig.2. The cloud-induced reduction in  $T_b$  depends on the amount of cloud ice, or IWP, in the upper troposphere. A  $T_b$  reduction is more readily seen at the spectral windows than near the atmospheric line features, because atmospheric gaseous absorption tends to attenuate the cloud scattering effects that come from the troposphere. In the case of a very strong atmospheric absorption, such as those from O<sub>2</sub> where the absorption occurs in the stratosphere, the MW radiation has little sensitivity to clouds or any emissions in the troposphere. The spectral window near 883 GHz is perhaps the highest band in MW to effectively measure cloud-included  $T_b$  reduction, beyond which the cloud scattering effect starts to decrease due to the increasing continuum absorption.

Ozone emission lines are not plotted in the full spectrum [Fig.2a], because they are everywhere in this spectral region. However, atmospheric ozone does produce absorption that would attenuate cloud scattering signals observed from space, therefore its effects were accounted for designing a cloud observing system. As shown in the detailed spectrum near 883 GHz in Fig. 2 (b and c), the design of IceCube cloud radiometer chose the local oscillator (LO) frequency at 883 GHz, such that its upper (892 GHz) and lower (874 GHz) sidebands are both located within a window of ozone absorption lines.

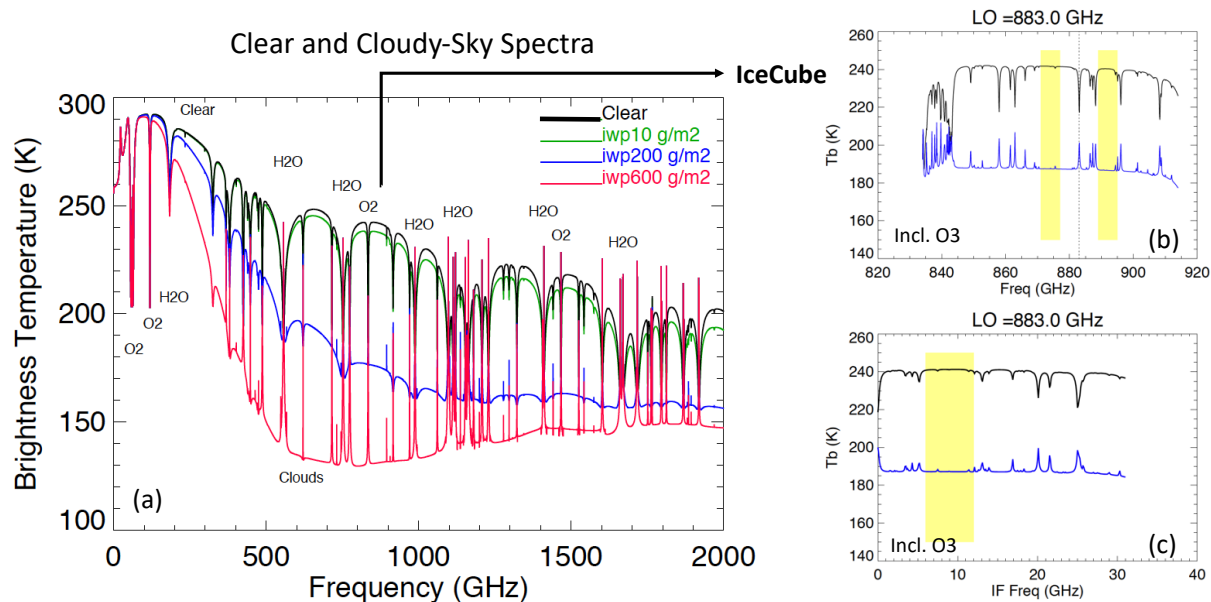


Fig. 2. (a) Cloud ice scattering at mm- and submm-wave frequencies from different IWPs. The 800-900 GHz region, one of the spectral windows where there are a fewer absorption line features from major atmospheric gases (i.e., O<sub>2</sub> and H<sub>2</sub>O), allows radiation to penetrate deeper into the atmosphere for cloud ice measurements. The higher frequency channel is more sensitive to cloud scattering than those at lower frequencies. Beyond 1 THz, the increasing H<sub>2</sub>O continuum absorption begins to attenuate the cloud scattering. (b) Detailed spectrum at 830-910 GHz that includes O<sub>3</sub> absorption lines. IceCube is designed to minimize impacts of atmospheric O<sub>3</sub> variability by setting the local oscillator frequency at 883 GHz. The yellow strips denote the receiver's upper and lower sidebands. (c) The IF spectrum in the IceCube's double-sideband receiver. The yellow strip denotes the IF band of IceCube.

## 1.2 The 883-GHz Cloud Radiometer

The 883 GHz receiver technology flown on IceCube was initially developed by VDI under a Small Business Innovation Research (SBIR) Phase II contract (NAS5-02107). Since the completion of Phase II in 2004, VDI has been successfully commercializing this technology. VDI has built over 100 receivers and sold over a dozen Vector Network Analyzer (VNA) Extenders in the 600 to 900 GHz frequency bands. GSFC worked previously with VDI in adapting its COTS 183 GHz receiver technology for the Global Precipitation Mission's Microwave Imager (GMI).

The IceCube 883 GHz radiometer technology is assessed at the system, sub-system, and component levels. The VDI-based 874 GHz radiometer system on CoSSIR is the first and only system known to us to have operated and observed the atmosphere to measure cloud ice from an aircraft [7]. The sub-system comprises a LO amplifier/multiplier chain (AMC) and mixer, which both VDI and JPL have demonstrated at TRL 5 [8][9][10]. AMC components in the 100-400 GHz range (IceCube requires a 441.5 GHz output) are developed by several organizations and are critical for radio astronomy in addition to remote sensing. Typically, planar Schottky varactor diodes have been used for multipliers, as is the case for the candidate VDI technology and for multipliers developed by JPL [11]. For the mW-level output power capability required here, the TRL is 5; however, lower power output circuits have flown in space for pumping superconductor-insulator-superconductor (SIS) mixers on ESA's Herschel Space Observatory. This latter technology is not appropriate for NASA Earth remote sensing missions because of its cryogenic requirements. Among room temperature Schottky diode mixer components, there were only three designs at 874 GHz prior to IceCube: VDI's sub-harmonic mixer [9]; JPL's sub-harmonic mixer [8]; and JPL's fundamental balanced mixer [10]. Each of these achieved TRL 5 (relative to spaceflight), although via different means. The latter two have been laboratory tested at room and cryogenic temperatures. Of the three, VDI's is the only one commercially available.

Because of the potentially high technical risk and development cost of submm-wave receivers, adapting VDI's COTS receiver technology for spaceflight offers a clear path for reducing risk and cost. The CoSSIR experience using COTS components suggested that only minimal changes were required for the meeting spaceflight-quality standards.

The key technology in the 883 GHz receiver (mixer, doubler, and tripler) had achieved TRL 5 through the high-altitude partial vacuum environment of the ER-2 flights which were over a wide temperature range. This was not sufficient to achieve TRL 6 for spaceflight qualification testing (operational environment). The least mature technology from a flight perspective is the tripler and V-band power amplifier at TRL 5, which is fabricated at BAE Systems with a flight-qualified InP process for the National Radio Astronomy Observatory (NRAO). IceCube uses these components to save significant DC power (3W) in the LO chain compared to the original CoSSIR design. The same parts are used operationally in the ALMA (Atacama Large Millimeter/tarubmillimeter Array) telescope at 16,500 ft in the Atacama Desert plateau in northeastern Chile. The other IceCube cloud radiometer components are at TRL 6 or higher. The custom designed interface card utilizes screened parts that were procured through GSFC’s electronic parts organization and leveraged existing flight project inventories. Technical risks of an electronics failure were further reduced with careful parts screening and thorough system level testing.

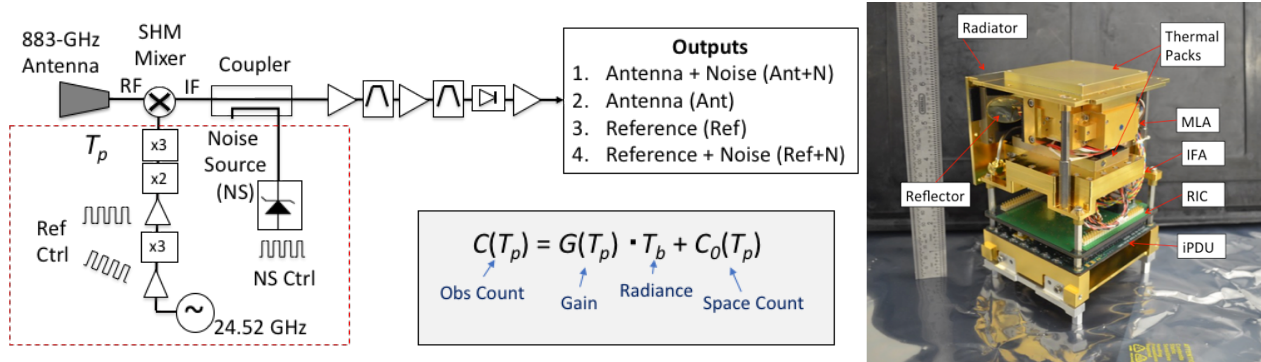


Fig.3. Block diagram of the IceCube 883 GHz receiver. The IF calibration includes noise source injection (“Ant+N” and “Ref+N” states), LO modulation (switching between “Ant” and “Ref” states), and LO power monitoring isolates the response of submm receiver components. The thermal environment of the receiver system is monitored by a thermistor near the mixer (T<sub>p</sub>). Measurements of four receiver states (Ant+N, Ant, Ref and Ref+N), sequencing through a 40ms time interval, are all output to diagnose the internal receiver noise as well as the radiance measurements from antenna. The image shows the IceCube instrument flight model (FM) integrated in a 1.5U volume, containing reflectors, MLA (Mixer LO Assembly), IFA (Intermediate Frequency Assembly), iPDU (instrument Power Distribution Unit), RIC (Receiver Interface Card), radiator and thermal paraffin packs.

A block diagram of the IceCube cloud radiometer system is shown in Fig.3 with key instrument performance parameters listed in Table 1. The RF receiver is comprised of an offset parabola reflector with feedhorn, mixer, stable oscillator, RF multiplier chain, IF chain, video amplifier and detector. There are also supporting circuit boards including the instrument power distribution unit (iPDU), receiver interface card (RIC), and command and data handling (C&DH), which is shared with the CubeSat. There is no moving part in this radiometer. The radiometric calibration is achieved by spinning CubeSat at a rate of ~1° per second to yield periodic views between cold space and Earth. The modeled clear-sky radiances from Earth’s atmosphere are used to provide the absolute radiometric calibration.

A block diagram of the IceCube cloud radiometer system is shown in Fig.3 with key instrument performance parameters listed in Table 1. The RF receiver is comprised of an offset parabola reflector with feedhorn, mixer, stable oscillator, RF multiplier chain, IF chain, video amplifier and detector. There are also supporting circuit boards including the iPDU and C&DH, which is shared with the CubeSat. There is no moving part in this radiometer. The radiometric calibration is achieved by spinning CubeSat at a rate of ~1° per second to yield periodic views between cold space and Earth. The modeled clear-sky radiances from Earth’s atmosphere are used to provide the absolute radiometric calibration.

In addition, the IceCube receiver experiment contains an internal IF calibration by operating the receiver frontend in a non-conventional way, imposing a 50% duty cycle on both the LO and noise source modulation (“Switching Sequence” in Fig.3). IF calibration is achieved by noise injection and LO power modulation (and monitoring), providing the means of discriminating the calibration state of frontend components referenced to space-view observations. The instrument temperature fluctuations can affect the gain and noise figure of the IF-chain, excess noise ratio of the IF noise diode, LO-drive power, and the subharmonic mixer (SHM) conversion loss, thus, posing significant challenge to tracking the system response. By incorporating frequent two-point IF calibration, LO power monitoring and periodic observations of deep space with switched noise source injection, this instrument design allows us to track and validate the instrument

response. In nominal operation, the instrument cycles through four measurement states in each 40-ms period: antenna (*Ant*), antenna + noise (*Ant+N*), IF reference (*Ref*), and IF reference + noise (*Ref+N*). Rather than using an IF switch, the LO power is modulated to effectively isolate the IF section. A noise source is coupled into the IF path during IF calibration and antenna measurements, thus, providing an RF-to-IF reference transfer. Four temperature sensors are used to monitor the thermal environment of sensitive components.

The radiometer frontend is comprised of a VDI's 883 GHz SHM pumped by a 441.5 GHz LO, which produces the lower and upper sidebands at 874 and 891 GHz respectively. The LO is sourced by 24.53-GHz (K-band) stable dielectric resonator oscillator (DRO), which is amplified and multiplied by a multichip module (MCM) containing a K-Band power amplifier MMIC, and frequency tripler and V-band power amplifier (PA) MMICs designed by NRAO/BAE for Atacama Large Millimeter wave Array (ALMA) telescope. This configuration saves 3W of DC power compared to the original CoSSIR design. The power output from this LO MCM drives the VDI frequency doubler and tripler, providing the ~2 mW required to pump the SHM. LO power is monitored at the second PA output using an inline microstrip directional coupler and V-band power detector.

The output of the mixer drives the IF chain (6-12 GHz), comprising an internal broadband noise source coupled into the IF path for calibration, followed by an isolator, LNA, band-pass filter, another gain stage, detector and video amplifier. The IF noise source uses components from the GMI X-band noise source design and the coupler and bandpass filter is designed and fabricated on the same standard microwave/RF substrate material using microstrip circuit topology. The video amplifiers are adopted from the Aquarius radiometer.

The antenna is an offset-fed paraboloid with a 15-mm aperture to produce a 1.8° half-power beamwidth, or 12.6 km footprint at nadir for the ISS orbit altitude (~400 km). Antenna beam spillover inside the instrument housing is minimized with absorber material placed on all critical flat surfaces. Its aperture is covered by a radome that is highly transparent in submm-wave but very reflective in infrared, to minimize impacts of external heat sources on the receiver.

Table 1. IceCube Radiometer Parameters

|                     |   |
|---------------------|---|
| Reflector Antenna   | Beam width: 1.8°; Beam efficiency: 93%      |
| MLA LO ( $f_{LO}$ ) | 883 GHz                                     |
| MLA noise temp      | 3842 K @20°C                                |
| IFA BW              | 6.5 GHz                                     |
| RIC                 | 10 kHz 14-bit ADC                           |
| Normal operation    | 50% LO cycle                                |
| NEDT (1-second)     | 0.3 K                                       |
| Mass                | 1.3 kg                                      |
| Daily Data Volume   | 24 MB (daytime), 48 MB (full day)           |
| Total DC Power      | 5.6 W (50% LO cycle); 7.4 W (100% LO cycle) |
| Subsystem           | 3.55 W (MLA); 1 W (IFA);                    |
| DC Power            | 2.5 W (iPDU); 0.3 W (RIC)                   |

Note: LO (local oscillator), MLA (Mixer LO Assembly), IFA (Intermediate Frequency Assembly), iPDU (instrument Power Distribution Unit), RIC (Receiver Interface Card), noise equivalent differential temperature (NEDT), bandwidth (BW).

The 883-GHz mixer was delivered with a noise temperature of <5000 K at 20°C over the entire 6-GHz IF bandwidth. Including some conversion losses in the IF chain, the radiometer's NEDT is measured at ~0.3 K for a 1-second integration time in the laboratory. This receiver sensitivity is measured at ambient temperatures up to ~35°C before it degrades significantly. It is important to verify the IceCube cloud radiometer performance over a wide range of temperatures. Although the instrument should ideally operate at 20 ±2°C, using paraffin packs in the CubeSat to stabilize the thermal environment, heat generated from the instrument and spacecraft often saturates the capacity of paraffin packs. As a result, cycling the instrument on and off is needed to prevent the instrument from reaching a very hot temperature. Nevertheless, a large (10°C to +37°C) range of instrument temperature variations is typically experienced in the daily IceCube operation.

### 1.3 CubeSat System

Because of the compact design and modest power draw of the 883-GHz cloud radiometer, the entire system can be hosted on a 3-U CubeSat. IceCube's spacecraft is built internally at GSFC using COTS components (Table 2). As shown in Fig.3, the bus consists of a 1.5U frame with the Attitude Determination and Control Subsystem (ADACS) attached to one end to complete a 2U unit. The ADACS is the XACT attitude control system from Blue Canyon Technologies (BCT). The BCT XACT has two modes: Sun Point (SP) and Fine Reference Point (FRP). SP is a safe mode to maintain spacecraft safety, while FRP is a high-performance mode for actual mission operations. The SP mode uses a minimal sensor suite to point a desired body-frame vector at the Sun, whereas the FRP mode uses the full sensor suite (e.g., GPS and star tracker) to accomplish a wide array of pointing objectives. The SP mode uses a coarse Sun sensor (CSS) as an absolute attitude reference to hold the spacecraft within 5° with respect to the Sun. The XACT 3-axis magnetometer is critical to momentum control in SP mode. In contrast, in FRP mode the momentum field is deduced from onboard time and ephemeris using a high-precision model of geomagnetic field.

Table 2. IceCube CubeSat (3U) Parameters

|                      |   |             |
|----------------------|---|-------------|
| Flight Configuration | Spinning Axis: Sun Vector (day); Magnetic Field (night) |             |
| ADACS                | BCT XACT  |             |
| L3 Cadet             | 1 W (Tx Power), 450/468 MHz (Rx/Tx Frequency)           |             |
| Ground Station       | WFF UHF   |             |
| Mass (w/ payload)    | 4.4 kg  |             |
| Data Storage         | 4 GB  |             |
| Data Rates           | Housekeeping:   | 173 bytes/s |
|                      | Science:  | 562 bytes/s |
|                      | System:   | 10 bytes/s  |
|                      | Total:  | 744 bytes/s |
| Clyde Space EPS      | 40 Whr (Battery)  |             |
| Operation Power      | 8.4 W (Average), 18 W (Est. Max)                        |             |
| Subsystem            | 4.4 W (XACT), 0.5 W (EPS), 0.8 W (GPSAnt),              |             |
| DC Power             | 0.9 W (GPSRec), 1.7 W (SIC), 0.1 W (Pumpkin)            |             |
| Design Lifetime      | 28 days   |             |

The overall IceCube system with payload fits within the 3U specification, with a total length of 340.5 mm, including 6.5mm posts on both ends, and a 100-mm by 100-mm body frame. Having the 3U split into bus and payload units takes full advantage of the CubeSat modular design, and the relatively minor volume inefficiency is offset by the ample volume margin available for subsystem boards. Bus components are also identified in Fig.5. The current configuration leaves a 56mm axial margin (25+31mm) from the possible 340.5mm 3U CubeSat specification (20% margin). The stowed double-sided solar panels protrude 8mm from the 100mm CubeSat limit on either side and comply with the NanoRacks launcher dimension requirement.

IceCube has a 4.4kg mass and takes in ~18W power from its solar panels. Nonetheless, power management is an operational challenge because of the large DC power draw from the 883-GHz cloud radiometer. Reducing its duty cycle on the LO modulation helps to lower the payload power. In addition, the CubeSat is required to keep its solar panels towards the Sun and operate the instrument during daytime only, to give a sufficient margin to battery lifetime for a 28-day technology demonstration. An orbital power management scheme from beginning of life (BOL) to end of life (EOL).

Rigorous tests were carried out to encompass standard CubeSat requirements as well as the requirements for rideshare to ISS. Specific tests included vibration testing of the CubeSat to encompass the launch environment and thermal vacuum cycling over expected operating temperature range. The system did not perform any self-compatibility EMI/EMC testing due to schedule and budgetary constraints, but did pass an end-to-end communication test with the ground station.

During a 5-day system-level thermal vacuum (TVAC) test, IceCube successfully deployed its solar panels and powered on the instrument for its performance verification. The cloud radiometer was calibrated using three blackbody references at +40°C, -40°C and -179°C (LN2). But the LN2 reference had malfunctioned due to a leakage problem. As a result, the radiometer performance was verified radiometrically with two references at +40°C, -40°C during pre-launch system-level environmental tests. The TVAC measurements were made for operational temperatures between 15°C and 25°C, providing an initial estimate of temperature-sensitive coefficients for the instrument calibration.

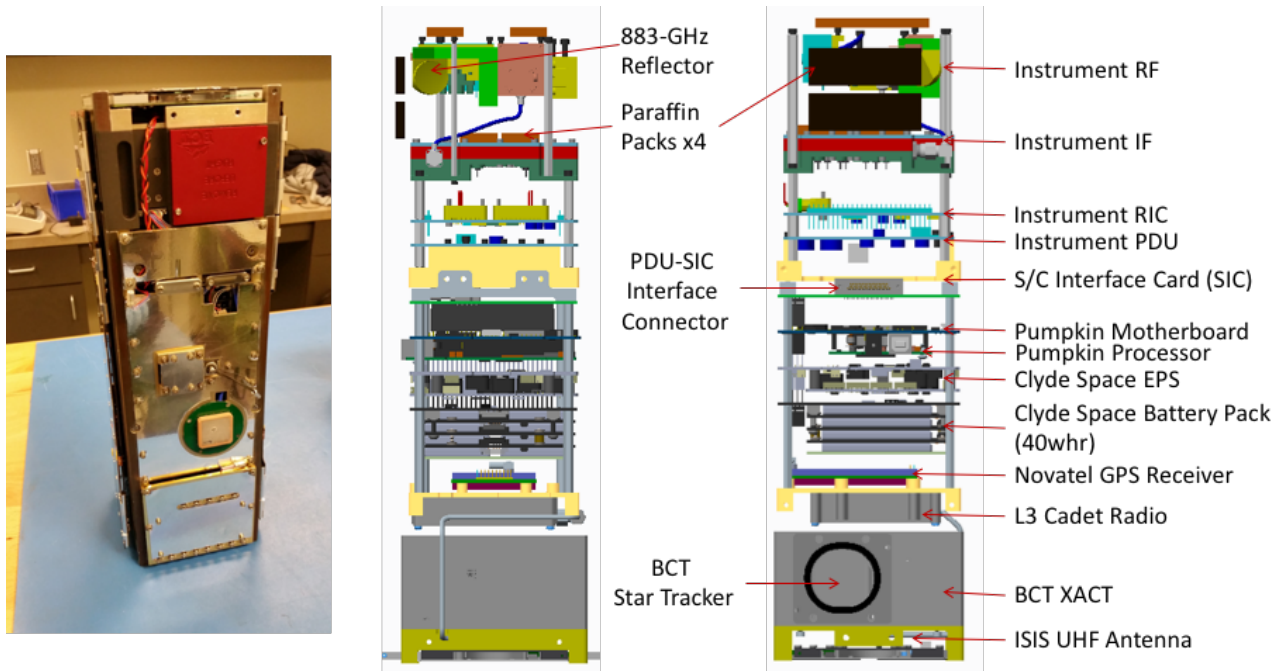


Fig.4. Integrated IceCube 3U CubeSat (left), and interior layouts of spacecraft (S/C) structure and key subsystems (right).

#### 1.4 Concept of Operations (ConOps)

IceCube’s flight software operates in three modes: deployment mode (DM), safe hold mode (SH), and science mode (SM). Successfully executed shortly after IceCube was released from ISS, DM represents the startup functionality of spacecraft, beginning with flight computer booting and ending with the spacecraft in SH. SH represents both the minimum functionality necessary to maintain and monitor spacecraft health and the mode in which the spacecraft communicates and responds to ground commands. All troubleshooting activities are conducted in this mode. SH is entered either when ground commands are sent to spacecraft, battery voltage drops below 7.5V or instrument radiator temperatures are outside of survival conditions. SM is the software mode in which spacecraft autonomously measures and records science data either during daytime, or through a pre-defined thermally-controlled instrument operation. The spacecraft must be ground-commanded into SM when in SH. The spacecraft transitions back to SH whenever a ground command is received. It can also transition back to SH autonomously in response to out of range battery voltage or instrument temperature violation. The spacecraft transitions directly from SM to DM if the flight computer automatically performs a soft or hard reset.

IceCube ground communications come through the GSFC WFF 18-m UHF dish. Although the IceCube radio is capable of transmitting at a rate of 1.5Mbps, the effective downlink data rate at WFF was ~0.2 Mbps on average during mission operation. There were usually 2-4 daily passes over WFF, producing an average of ~3 contacts per day. Routine operation at WFF was, however, limited to daytime hours on weekdays. The average contact time was ~10 min with a successful rate of 76%, of which ~55% had successful responses to ground-station requests. Because of the IceCube’s low data volume, the onboard 4GB memory allowed most of the science data stored onboard to be downlinked on a weekly basis.

IceCube flew in a 52°-inclination orbit similar to ISS, with an initial orbital apogee of 416 km and perigee of 402 km. Each orbit had ~50 min of sunlight time. Because the flight thermal condition and solar power input vary highly with

orbital geometry (e.g., beta angle), the initial ConOps was to keep the instrument off, allowing assessment of CubeSat health and establishment of optimal parameters for safe mission operation through both day and night. Two parameters were closely monitored; battery voltage ( $V_b$ ) where  $V_b$  should be greater than 7.5V (vs. normal 8.1V), and payload temperature ( $T_p$ ) which should be less than 40°C.

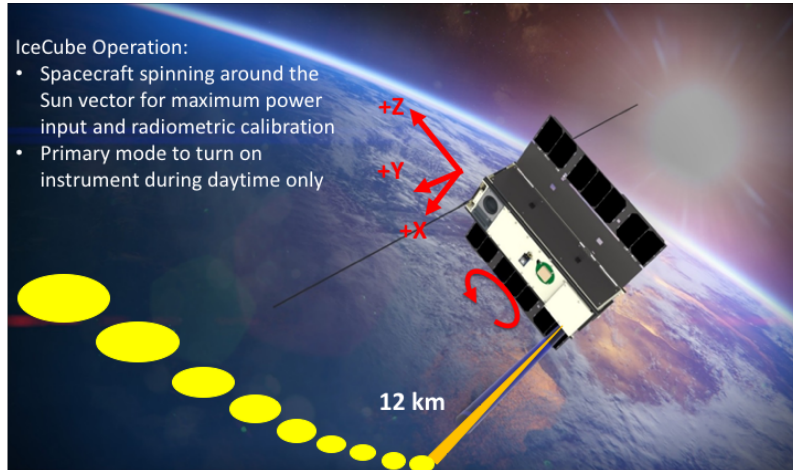


Fig. 5. IceCube concept of operation (CONOP). Illustrated is the IceCube’s spacecraft spinning around the Sun vector, to maximize solar power input during the spaceflight while allowing periodical views of Earth and cold space for radiometric calibration. The nadir footprint size is ~12km

IceCube demonstrated spin stabilization using the BCT XACT system. It has been spun at various rates between 0.2 and 3.3 degrees per second (dps). During the early period of the mission, the FRP mode with a spin rate of 1.2 dps was employed. At this rate, the star-tracker was able to acquire good navigation data while the spacecraft spun. However, there has been an issue in the FRP operation to keep GPS locked to the star-tracker continuously. In the event of unlocking, a reset command has to be sent to the spacecraft, to re-initiate the FRP operation. Since unlocking events occurred frequently, the FRP operation reset was abandoned during operation after October 2017, leaving most of the observations from the SP mode in the recent months.

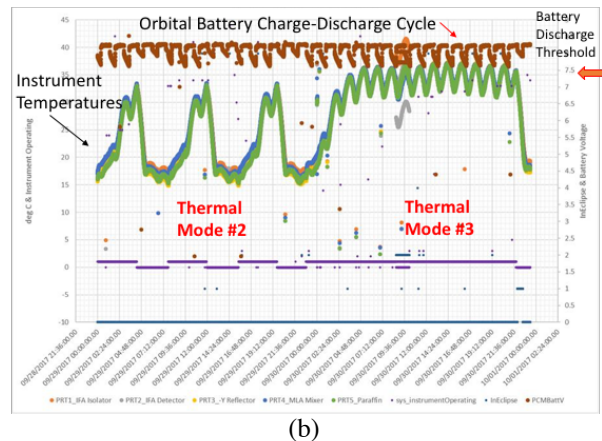
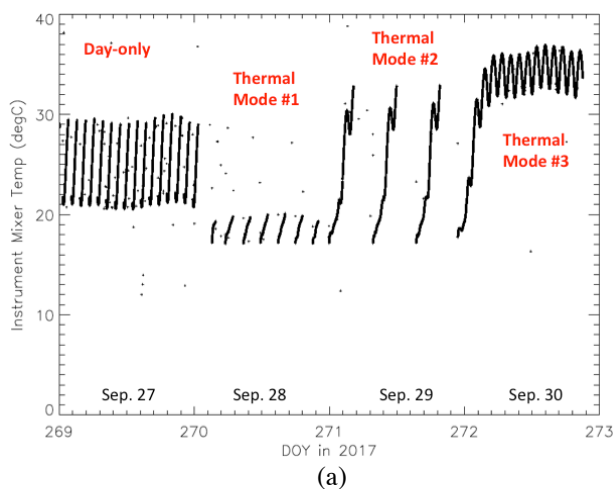


Fig.6. (a) IceCube  $T_p$  from four operational experiments with the instrument powered on and off at different time intervals. The thermal-mode #3 is the 24/7 science operation when  $T_p$  reached an equilibrium of 34-38°C. (b) Detailed temperature and battery voltage variations during the 24/7 operation, showing that the voltage stayed above the 7.5V threshold and all instrument temperatures plateaued at 38°C. The thermal test #3 confirms that the 40-Whr battery can support full-day operation of the 5.6W payload.



During daytime the spacecraft spins around the Sun vector (-Y axis) to produce maximum solar power while allowing the radiometer to be calibrated periodically [Fig.5]. This operation is called the daytime-only science mode (DO-SM), in which BCT XACT spins around -Y axis at a rate of 1.0 dps in the SP mode or around +Z axis at 1.2 dps in the FRP mode. The XACT performs attitude determination autonomously. The Kalman attitude filter operates constantly in the background (even in the SP mode). The algorithm would not return a valid attitude until a valid attitude measurement has been obtained from the star tracker. If the tracker ceases to provide valid attitude measurements, the onboard attitude remains valid for a table-valued duration (nominally 1 hour) as long as the inertial measurement unit (IMU) measurements are available to propagate it. The bias stability of the XACT IMU is  $\sim 3$  degrees over an hour.

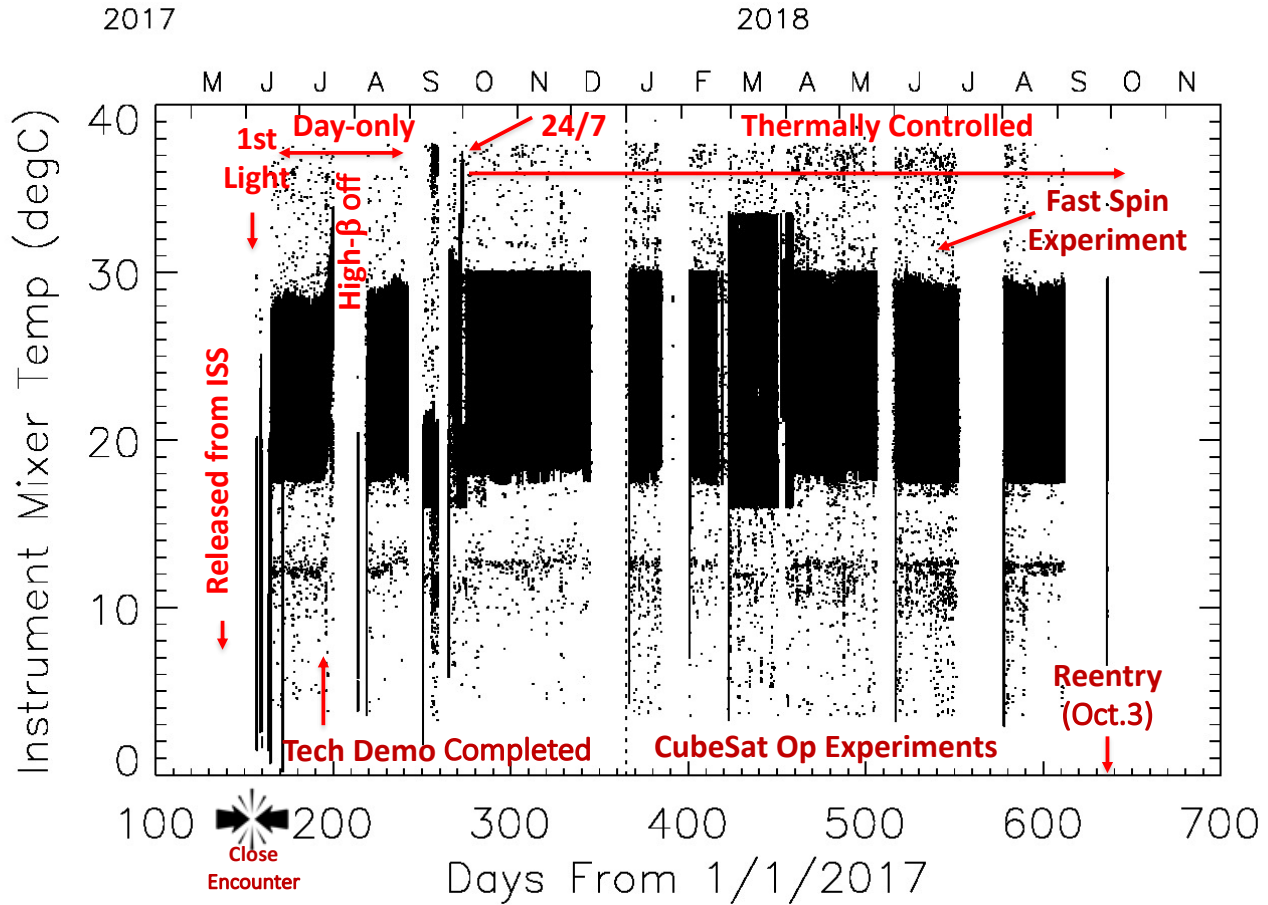


Fig. 7. IceCube T<sub>i</sub> variations during different operational modes/experiments since launch. IceCube had a close encounter but avoided the collision with another CubeSat shortly after released from ISS. The coldest temperature is  $\sim 2^{\circ}\text{C}$  when the instrument was powered off for a long period of time. The warmest temperature ( $\sim 38^{\circ}\text{C}$ ) occurred when the cloud radiometer was powered on continuously for 24 hours. The operation was thermally controlled after Oct 2017 with T<sub>i</sub> capped at  $30^{\circ}\text{C}$ .

At night IceCube relies on its onboard magnetometer to align the spacecraft's +Z axis along the geomagnetic field. The spacecraft spins around the +Z axis at a rate of  $\sim 1.5$  dps at night. The battery discharges gradually after the spacecraft enters eclipse, but need to maintain an output voltage above 7.5V in order to avoid over-discharging. During the initial operation a conservative approach was adopted by powering on the instrument only during daytime, to assure the battery adequately charged all the time during the 28-day technology demonstration period (i.e., primary mission).

On September 30, 2017 IceCube successfully conducted a 24/7 experiment for the full-power cloud radiometer operation. Using its double-sided solar panels and 40 Whr battery, the CubeSat can support a 5.6 W payload for full-time operation. With this mode, basically, the 883-GHz radiometer is left on all the time, which produces the most stressful operation on the spacecraft battery. It was first used on June 8 for two consecutive orbits. Since the operation time was short, the instrument did not reach its thermal equilibrium and the battery stress was not long enough to verify its

capability. It was tested again on September 30 for approximately one day when the instrument reached a thermal equilibrium of  $\sim 38^\circ\text{C}$  [Fig.6], which is still below the limit ( $40^\circ\text{C}$ ) for safe instrument operation. In this experiment the battery voltage never dropped below 7.5V, confirming that the 40 Whr battery can support the 24/7 operation of the 5.6-W payload. Because the 883-GHz radiometer becomes much noisier above  $35^\circ\text{C}$  for cloud observations, 24/7 operation was modified to keep the instrument on only below  $30^\circ\text{C}$ . This operation is called thermally-controlled science mode (TC-SM), such that the instrument is automatically powered off when  $T_r$  reaches  $30^\circ\text{C}$  and powered back on when  $T_r$  drops to  $18^\circ\text{C}$ . The TC-SM operation is a fully autonomous mode and has been employed since October 2017.

The spacecraft and instrument thermal environments play an important role in operating the 883-GHz cloud radiometer. As shown in Fig.7 the DO-SM operation yielded a relatively stable orbit-to-orbit thermal range ( $18^\circ\text{C}$  -  $29^\circ\text{C}$ ) for  $T_r$  when the beta angle is normal. Note that the time in eclipse, when the spacecraft cools, gets shorter as beta angle increases, and can go to zero (no eclipses) as beta angle approaches  $90^\circ$ . During a high beta-angle period (e.g., July 20 – Aug 10, 2017),  $T_r$  rose quickly and the instrument was powered off. During the DO-SM operation, the instrument was on for  $\sim 58\%$  time of the orbit period. A drawback of the DO-SM operation is that it requires the special care needed to monitor the instrument temperature in the high beta-angle condition. Therefore, a thermal-controlled operation was developed and implemented to achieve fully autonomous operation. Fig.7 also reveals the days when the cloud radiometer was restarted from a power-off. After the instrument is powered off, its temperature usually drops below  $10^\circ\text{C}$ , indicating the instrument turn-on days.

## 2. CLOUD OBSERVATIONS

As with other nadir/slant/limb viewing microwave sensors [12][13][14][15][16], ice cloud detection requires significant contrast between the cloudy- and clear-sky radiances. This difference is also called cloud-induced radiance ( $T_{cir}$ ). We compute the 883-GHz  $T_{cir}$  from the observed radiance ( $T_o$ ) and the clear-sky radiance ( $T_c$ ) from the radiative transfer model as described above, i.e.,  $T_{cir} = T_o - T_c$ .

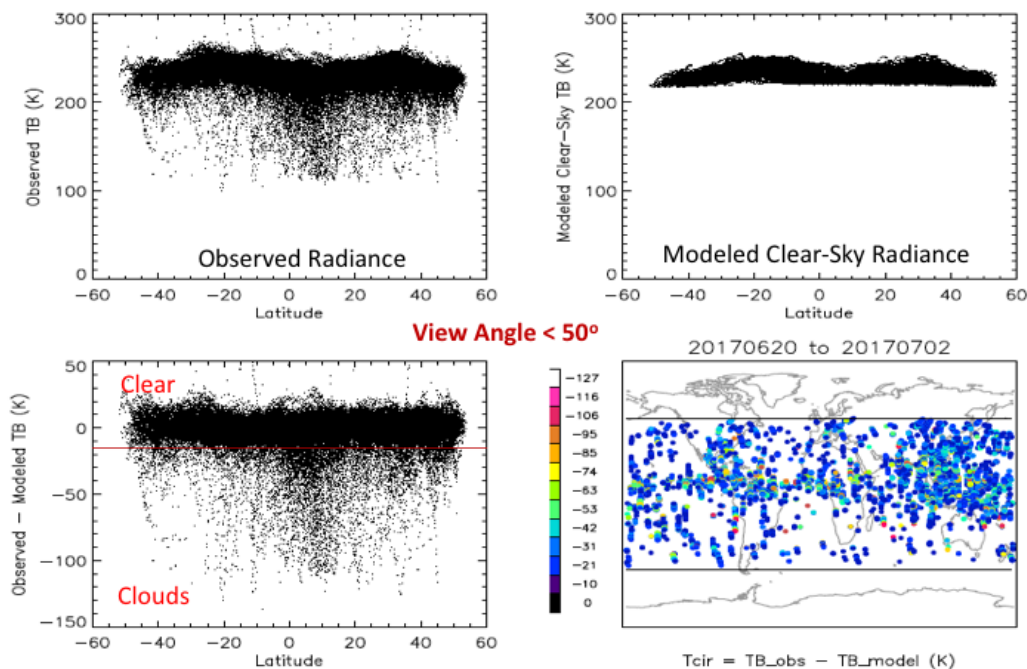


Fig. 8. Cloud detection with IceCube 883-GHz radiances. The top panels show the observed and modeled radiances, from which  $T_{cir}$  are computed as their difference. Only data with view angle  $< 50^\circ$  are used. The  $T_{cir}$  below the threshold of -15K (red line) indicate significant cloud scattering. The distribution of flagged  $T_{cir}$  is shown on the right-bottom panel. IceCube has a latitude coverage between  $52^\circ\text{S}$ - $52^\circ\text{N}$ , similar to the ISS orbit.

A threshold of -15 K, approximately  $3\sigma$  of the  $T_{cir}$  variability in clear sky, is applied to IceCube  $T_{cir}$  to flag the significant radiance depression due to cloud scattering [Fig.8]. The  $3\sigma$  clear-sky  $T_{cir}$  variability was suggested as a reliable threshold to minimize false cloud detection [14]. In spaceborne cloud remote sensing,  $T_{cir}$  variability is often dominated by systematic errors associated with the modeled clear-sky radiance  $T_e$ . In the IceCube case, the radiance measurement error is comparable with  $T_e$  errors, because of radiometric calibration challenges.

The detected  $T_{cir}$  are further converted to  $pIWP$  using a modeled  $pIWP$ - $T_{cir}$  relation that can be derived from the radiative transfer model [17], where  $pIWP$  is a partial column of cloud  $IWP$ . Wu et al. [4] compared the cloud ice observed by passive MW sensors with CloudSat measurements, and concluded that none of the passive sensors from space can measure the entire column of cloud ice, especially in the presence of thick-and-dense clouds. Strong extinction from clear-sky absorption and cloud scattering prevents the radiation from penetrating deep into these clouds, causing saturation in cloud ice sensitivity. It is this saturation that yields a partial column  $pIWP$  and must be taken into account when comparing cloud ice measurements from different sensors.

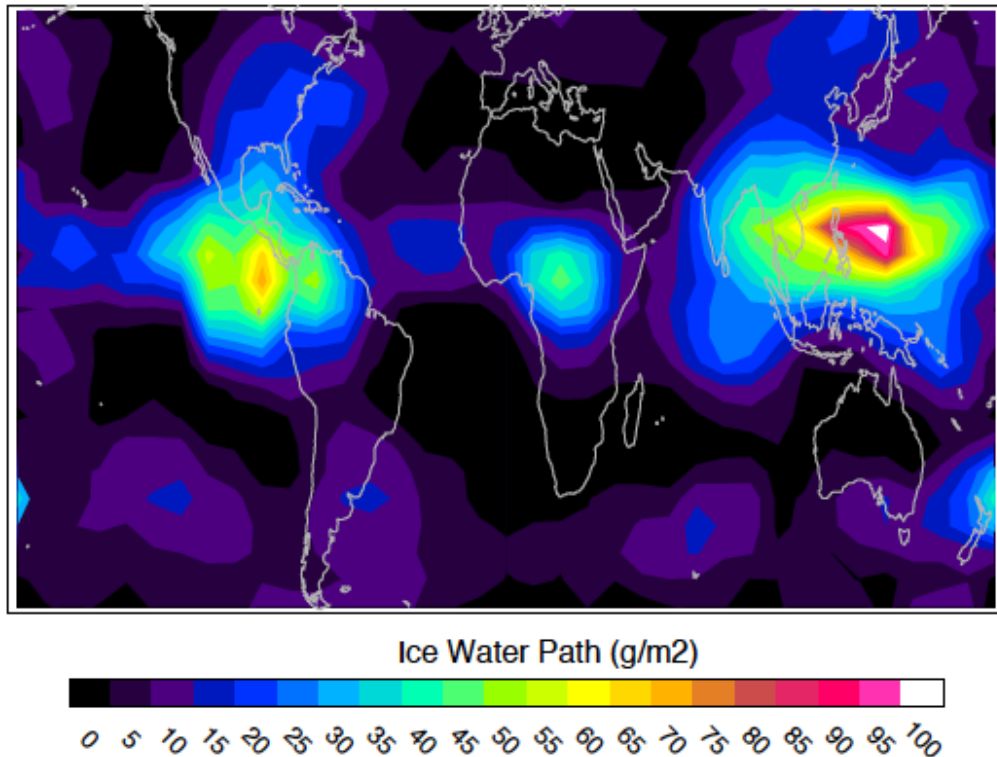


Fig. 9. IceCube 883-GHz cloud  $pIWP$  map for July-September 2017 at latitudes between  $52^{\circ}\text{S}$ - $52^{\circ}\text{N}$ . A longitude-latitude grid of  $10^{\circ}\times 5^{\circ}$  is used for computing the map. As in Fig. 15,  $T_{cir}$  is discriminated with the -15K threshold, and only measurements with  $T_e < 30^{\circ}\text{C}$  and view angle  $< 50^{\circ}$  from nadir are used.  $T_{cir}$  is further converted to  $pIWP$  in  $\text{g}/\text{m}^2$  using a modeled  $pIWP$ - $T_{cir}$  relation, as in the MLS cloud ice retrieval.

A key parameter that characterizes  $pIWP$  is the bottom height of the partial column, which can be roughly estimated from the modeled clear-sky radiances using atmospheric temperature lapse rate (7.5 km) [Table 3]. These clear-sky MW  $T_e$  represent, to the first order, the upper-tropospheric blackbody emission: the colder the MW  $T_e$ , the higher the emission height. For example, the Microwave Limb Sounder (MLS) 640-GHz clear-sky  $T_e$  is  $\sim 205\text{K}$  in the tropics, which corresponds to a blackbody temperature of  $T=220\text{K}$ . Assuming an atmosphere with the scale height of 7 K/km and a surface temperature  $T_s=300\text{K}$ , one would obtain a bottom height of  $\sim 11$  km for the 640-GHz limb sounding channel. By the similar token, the bottom height for IceCube 883-GHz cloud ice is  $\sim 8$  km, slightly lower than MLS 640 GHz but higher than MLS 240 GHz, which suggests that the 883-GHz cloud ice should fall between MLS 640 and 240 GHz  $pIWP$  in terms of column amount.

Table 3. Saturation Height of *pIWP* for Selected MW Channels

| Sensors         | Avg. <i>T</i> (K) | Atmos. <i>T</i> (K) | Est. Height (km) |
|-----------------|-------------------|---------------------|------------------|
| IceCube 883 GHz | 220               | 240                 | ~8               |
| MLS 118 GHz     | 220               | 222                 | ~10.5            |
| MLS 190 GHz     | 242               | 247                 | ~7               |
| MLS 240 GHz     | 240               | 246                 | ~7               |
| MLS 640 GHz     | 205               | 220                 | ~10.7            |

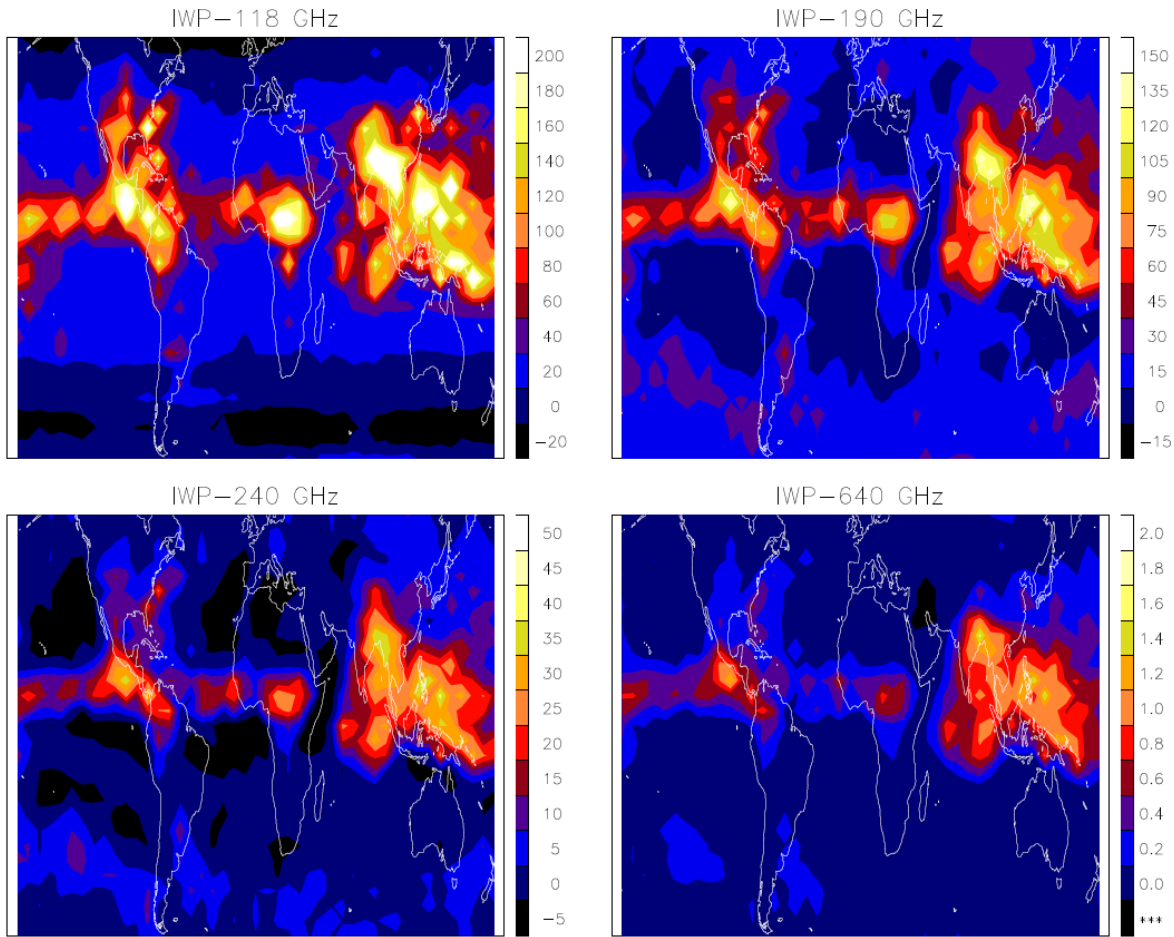


Fig. 10. Aura/MLS cloud *pIWP* maps for July-September 2017 in the same latitude range. Four MLS channels can observe cloud ice from limb sounding geometry, each of which corresponds to a different partial column height [Table 3]. In addition, the higher the frequency, the more sensitivity of MLS radiance to small cloud particle scattering. Combined effects from scattering sensitivity and penetration depth determine the observed *pIWP* [4].

The first global 883-GHz cloud ice map was obtained by IceCube during its operation in July-September 2017 [Fig.9]. It represents the unique upper-tropospheric cloud ice amount detected by a sensor that has sensitivity between traditional MW and IR instruments from space. The IceCube-measured cloud ice is a column amount roughly from heights above 8 km. Despite much fewer samples taken during this observation period, IceCube produces a cloud ice morphology similar to MLS *pIWP* maps [Fig.10], in particular, to the MLS 640 GHz, where both sensors have a similar frequency sensitivity to ice cloud scattering. There are three prominent peaks in the IceCube map that come from tropical deep convection in the intertropical conversion zone (ITCZ). The Pacific peak is strongest, followed by one over the central America and tropical Africa. The similar relative strengths are seen in the MLS 640 GHz cloud ice map.

Compared to the MLS *pIWP* in the extratropics [Fig.10], IceCube's 883-GHz radiometer observes more cloud ice than that from MLS 640 GHz but less than MLS 190 and 240 GHz observations. IceCube's nadir/slant viewing geometry and higher frequency (better sensitivity to smaller particles) gives it deeper penetration into the upper tropopause than MLS 640-GHz limb sounding. Therefore, the additional cloud ice seen by IceCube is consistent with the slightly deeper penetration in the extratropics. However, MLS 190 and 240 GHz channels, which make even deeper penetration (~7km), have larger *pIWP* values than IceCube in the extratropics as expected.

## SUMMARY

IceCube is the first CubeSat built by GSFC at the time (i.e., 2014) when commercial CubeSat providers were immature and only spacecraft subsystems and components were available. It was a pathfinder at NASA to put a 3U flight system quickly so as to demonstrate the commercial low-cost 883-GHz cloud receiver technology. Thus, the IceCube instrument and spacecraft development was on an unusually fast schedule (2.5 years) and tight budget, compared to normal NASA flight projects. The IceCube spacecraft integration and test revealed numerous reliability issues with COTS parts and subsystems, for which some re-engineering and rework were needed. Relying on NASA's system engineering approach, the project was able to identify and mitigate some of mission-critical risks through expert advice, vigorous testing in targeted subsystems/components, and small, swift working-group activities. IceCube was tested thoroughly as a "Class D-minus" mission in a flight-like thermal vacuum environment to verify instrument and system functionality. The final delivered system was a product with the top two risks in the mechanisms associated with solar panel deployment and battery inhibit switches.

IceCube demonstrated the CubeSat spinning capability at altitudes > 200 km with a spin rate as high as 3.3 dps. To maximize the spacecraft's power input, IceCube operation was configured to keep the solar panels facing at the Sun all times during the day. The spacecraft spins around the Sun vector during daylight and around the local magnetic field vector at night. The spin produces periodic views of cold space for radiometric calibration of the 883-GHz cloud radiometer.

The spaceflight performance of the IceCube spacecraft and instrument exceeded their expectations. The project met all mission objectives for 883-GHz technology demonstration, and continued to accumulate knowledge about long-term stability and performance of the CubeSat and the cloud radiometer. The 15-month flight data show that the 883-GHz commercial radiometer can last for a long period of time and maintain a good sensitivity at its designed operational temperature. Inflight operation experiments also confirmed that the 18-W IceCube EPS was able to support 24/7 operation of the 5.6-W payload. The 883-GHz radiometer can be powered on continuously without over-discharging its battery during eclipse. The instrument would reach an equilibrium temperature of  $T_p \sim 38C$  in the 24/7 mode. For good-quality cloud observations, IceCube operation employed a thermal-control mode since October 2017, in which  $T_p$  was capped at 30C.

The IceCube 883-GHz cloud radiometer was essentially a free-running receiver without internal calibration targets. It relied on periodic views between cold space and Earth. The spinning CubeSat provided frequent space views, which were sufficient to track and model the receiver's background count variations. The power-cycling MLA receiver operation allowed separation of the instrument frontend and backend noise contributions, and effective removal of complex backend noise variations in the Ant-Ref count differences. The 883-GHz radiances have been calibrated to ~3K. These calibrated radiances produced the first 883-GHz cloud ice map validated by MLS observations during the same period.

The successful IceCube spaceflight and submm-wave technology demonstration have enabled a new remote sensing capability for future cost-constrained science missions with:

- Low-cost, space-qualified instruments at frequencies up to 883 GHz;
- Fast-track exploration with focused science objectives; and
- Cost-effective implementation of a SmallSat/CubeSat constellation.

## REFERENCES

- [1] Evans, K. F., S. J. Walter, A. J. Heymsfield, G. M. McFarquhar, "Submillimeter-wave cloud ice radiometer: Simulations of retrieval algorithm performance," *J. Geophys. Res.*, 107, 2.1–2.21. (2002)
- [2] Buehler, et al, "Observing ice clouds in the submillimeter spectral range: the CloudIce mission proposal for ESA's Earth Explorer 8," *Atmos. Meas. Tech.*, 5, 1529–1549. (2012)
- [3] Stephens, G. L., et al., "CloudSat mission: Performance and early science after the first year of operation," *J. Geophys. Res.*, 113, D00A18, doi:10.1029/2008JD009982. (2008)
- [4] Wu, D. L., et al., "Comparisons of global cloud ice from MLS, CloudSat, and other cor-relative data sets." *J. Geophys. Res.*, (CloudSat special section), doi:10.1029/2008JD009946. (2009)
- [5] Eliasson, S., et al., "Assessing observed and modelled spatial distributions of ice water path using satellite data," *Atmos. Chem. Phys.*, 11, 375–391, doi:10.5194/acp-11-375-2011. (2011)
- [6] Zhang, Z. and B. Monosmith, "Dual-643 GHz and 874 GHz Airborne Radiometers for Ice Cloud Measurements," *IEEE Int. Geoscience and Remote Sensing Symposium (IGARSS)*, Boston, 7-11 July 2008, vol.2, pp.1172-1175. (2008)
- [7] Evans, K.F., et al., "Ice hydrometeor profile retrieval algorithm for high frequency micro-wave radiometers: application to the CoSSIR instrument during TC4," *Atmos. Meas. Tech.*, 5, 2277-2306. doi:10.5194/amt-5-2277-2012. (2012)
- [8] Hesler, J., "Compact Terahertz Heterodyne Receivers," *NASA SBIR Phase II Final Report*, Contract: NAS5-02107. (2004)
- [9] Thomas, B., et al., "Design of an 874 GHz biasable sub-harmonic mixer based on MMIC membrane planar Schottky diodes," In proceeding of 33rd International Conference on Infrared, Millimeter and Terahertz Waves. doi:10.1109/ICIMW.2008.4665424, (2008)
- [10] Thomas, B., et al., "A Broadband 835–900-GHz Fundamental Balanced Mixer Based on Monolithic GaAs Membrane Schottky Diodes," *IEEE Trans. Microwave Theory and Techniques*, doi:10.1109/TMTT.2010.2050181. (2010)
- [11] Schlecht, E., et al., "Capability of THz sources based on Schottky diode frequency multiplier chains," *Microwave Symposium Digest, IEEE MTT-S International*, 6-11 June 2004, vol.3, pp 1587-1590. (2004)
- [12] Zhao, L. and F. Weng, "Retrieval of ice cloud parameters using the Advanced Microwave Sounding Unit (AMSU)." *J. Appl. Meteor.*, 41, 384- 395. (2002)
- [13] Wu, D. L., W. G. Read, A. E. Dessler, S. C. Sherwood, and J. H. Jiang, "UARS MLS Cloud Ice Measurements and Implications for H<sub>2</sub>O Transport near the Tropopause," *J. Atmos. Sci.*, 62 (2), 518-530, (2005).
- [14] Wu, D. L., and Coauthors, "Validation of the Aura MLS cloud ice water content measurements." *J. Geophys. Res.*, 113, D15S10, doi:10.1029/2007JD008931. (2008)
- [15] Eriksson, P., M. Ekstrom, B. Rydberg, D. L. Wu, R. T. Austin, and D. P. Murtagh, "Comparison between early Odin-SMR, Aura MLS and CloudSat retrievals of cloud ice mass in the upper tropical troposphere." *Atmos. Chem. Phys.*, 8, 1937–1948, doi: 10.5194/acp-8-1937-2008. (2008)
- [16] Gong, J., and D. L. Wu, "CloudSat-constrained cloud ice water path and cloud top height retrievals from MHS 157 and 183.3 GHz radiances", *Atmospheric Measurement Techniques*, 7 (6): 1873-1890. (2014)
- [17] Wu, D. L., J. H. Jiang, and C. P. Davis, "EOS MLS cloud ice measurements and cloudy-sky radiative transfer model," *IEEE Trans. Geosci. Remote Sens.*, 44(5), 1156– 1165. (2006)